Title
Clinical validation of a nanodiamond-embedded thermoplastic biomaterial.

Journal
Proceedings of the National Academy of Sciences of the United States of America, 114(45)

ISSN
0027-8424

Authors
Lee, Dong-Keun
Kee, Theodore
Liang, Zhangrui
et al.

Publication Date
2017-11-01

DOI
10.1073/pnas.1711924114

Peer reviewed

Clinical validation of a nanodiamond-embedded thermoplastic biomaterial

Dong-Keun Lee[a,b,1], Theodore Kee[c,1], Zhangrui Liang[d,1], Desiree Hsiou[a], Darron Miya[a], Brian Wu[a], Eiji Osawa[e], Edward Kai-Hua Chow[f,g,h], Eric C. Sung[i,2], Mo K. Kang[d,2], and Dean Ho[a,b,c,j,k,2]

[a]Division of Oral Biology and Medicine, School of Dentistry, University of California, Los Angeles, CA 90095; [b]The Jane and Jerry Weintraub Center for Reconstructive Biotechnology, School of Dentistry, University of California, Los Angeles, CA 90095; [c]Department of Bioengineering, Henry Samueli School of Engineering and Applied Science, University of California, Los Angeles, CA 90095; [d]Section of Endodontics, Division of Constitutive & Regenerative Sciences, School of Dentistry, University of California, Los Angeles, CA 90095; [e]NanoCarbon Research Institute, Shinshu University, Ueda, Nagano 386-8567, Japan; [f]Cancer Science Institute of Singapore, Yong Loo Lin School of Medicine, National University of Singapore, Singapore 117599, Singapore; [g]Department of Pharmacology, Yong Loo Lin School of Medicine, National University of Singapore, Singapore 177599, Singapore; [h]National University Cancer Institute, Singapore 119082, Singapore; [i]Division of Advanced Prosthodontics, School of Dentistry, University of California, Los Angeles, CA 90095; [j]California NanoSystems Institute, University of California, Los Angeles, CA 90095; and [k]Jonsson Comprehensive Cancer Center, University of California, Los Angeles, CA 90095

Edited by Eun Ji Chung, University of Southern California Biomedical Engineering Department, Los Angeles, CA, and accepted by Editorial Board Member Mark E. Davis September 21, 2017 (received for review July 4, 2017)

Detonation nanodiamonds (NDs) are promising drug delivery and imaging agents due to their uniquely faceted surfaces with diverse chemical groups, electrostatic properties, and biocompatibility. Based on the potential to harness ND properties to clinically address a broad range of disease indications, this work reports the in-human administration of NDs through the development of ND-embedded gutta percha (NDGP), a thermoplastic biomaterial that addresses reinfection and bone loss following root canal therapy (RCT). RCT served as the first clinical indication for NDs since the procedure sites involved nearby circulation, localized administration, and image-guided treatment progress monitoring, which are analogous to many clinical indications. This randomized, single-blind interventional treatment study evaluated NDGP equivalence with unmodified GP. This progress report assessed one control-arm and three treatment-arm patients. At 3-mo and 6-mo follow-up appointments, no adverse events were observed, and lesion healing was confirmed in the NDGP-treated patients. Therefore, this study is a foundation for the continued clinical translation of NDs and other nanomaterials for a broad spectrum of applications.

nanodiamonds | nanomedicine | clinical trial | biomaterial | infection

The field of nanomedicine has developed several classes of promising nanomaterials, including polymers, metallic particles, nanocarbons, and other important platforms for applications that include drug delivery and imaging, among others (1–7). While multiple nanoparticles have been evaluated through in-human studies, there remains a need to accelerate novel, nanotechnology-enabled strategies that can enhance the efficacy and safety of therapy into the clinic (8, 9). Among these strategies are detonation nanodiamonds (NDs), which integrate multiple favorable properties into a single platform. For example, NDs possess uniquely faceted electrostatic properties that have mediated marked enhancements in drug delivery and imaging efficacy (10–24). NDs are highly scalable materials and byproducts of conventional mining and refining. Conventional ball milling and acid washing as well as other methods have previously been employed to realize uniform particles that are ready for biomedical applications (25–27). With regard to ND tolerance and biocompatibility, a large body of work has confirmed that they are well tolerated across in vitro and preclinical models. Of note, a recent nonhuman primate study was conducted where standard and elevated dosages and repeated administration over a 6-mo period revealed no apparent toxicity (28). The administration of NDs alone has also been shown to inhibit bacterial biofilm formation at dosages comparable to those of ampicillin (29, 30). ND-containing composite materials have also been shown to exhibit superior mechanical properties compared with unmodified materials (27, 31, 32). Harnessing these important ND attributes toward clinical implementation, this study reports the in-human administration of a ND-embedded gutta percha, a thermoplastic biomaterial that is used as a nonsurgical root canal therapy (RCT) filler material to prevent reinfection and enable lesion healing. RCT is a standard treatment used to address infected pulp tissue, composed of blood vessels and nerve tissue, within the tooth and protect the tooth against future reinfection, while preserving its function. Therefore, it is a procedure that is relevant to a broad range of clinical challenges with high prevalence ranging from wound healing to regenerative medicine and infectious diseases, among others that can be addressed using emerging technologies such as nanomedicine. There are over 15 million RCT procedures performed each year in the United States (33). There is a widespread need for RCT procedures since pulp tissue infection can result from a spectrum of issues

Significance

There is a continued need to advance novel nanomedicine platforms into the clinic to address treatment challenges in oncology, infection, and regenerative medicine, among other areas. As such, this work demonstrates the in-human validation of nanodiamonds through their incorporation into gutta percha [nanodiamond-embedded gutta percha (NDGP)], a polymer that repairs root canal treatment sites following tissue disinfection. A randomized, dual-arm clinical trial was implemented, and study endpoints included confirmation of lesion healing, postoperative pain reduction, and the absence of reinfection. To date, the NDGP-treated patients successfully met the study endpoints. Therefore, these findings support the potential expansion of nanodiamonds, and the broader nanomedicine field, into other disease indications.

Author contributions: D.-K.L., T.K., E.C.S., M.K.K., and D. Ho designed research; D.-K.L., Z.L., E.K.-H.C., E.C.S., M.K.K., and D. Ho performed research; D.-K.L. and E.O. contributed new reagents/analytic tools; D.-K.L., T.K., Z.L., D. Hsiou, D.M., B.W., E.C.S., M.K.K., and D. Ho analyzed data; and D.-K.L., T.K., Z.L., D. Hsiou, D.M., B.W., E.O., E.K.-H.C., E.C.S., M.K.K., and D. Ho wrote the paper.

Conflict of interest statement: E.O. is an inventor on US Patent No. 7300958 entitled "Ultra-dispersed nanocarbon and method for preparing the same." E.K.-H.C. and D. Ho are inventors on US Patent No. 20150238639 entitled "Contrast agent and applications thereof." D. Ho is an inventor on US Patent No. 20100305309 entitled "Nanodiamond particle complexes" and US Patent No. 9125942 entitled "Paramagnetic metal–nanodiamond conjugates." The other authors declare no conflict of interest.

This article is a PNAS Direct Submission. E.C. is a guest editor invited by the Editorial Board.

[1]D.-K.L., T.K., and Z.L. contributed equally to this work.

[2]To whom correspondence may be addressed. Email: esung@dentistry.ucla.edu, mkang@dentistry.ucla.edu, or dean.ho@ucla.edu.

This article contains supporting information online at www.pnas.org/lookup/suppl/doi:10.1073/pnas.1711924114/-/DCSupplemental.

including trauma, caries, and periodontitis. The purpose of RCT is to remove bacteria-infected neurovascular and pulpal tissues within a tooth, shape the canal space for the subsequent administration of a biocompatible filling material, establish a bacteria-tight seal, and promote healing of periradicular bone destruction to retain the natural tooth function (34, 35). Successful treatment outcomes are defined by the elimination of pain, reduced radiolucency of the originally infected bone tissue, a bacteria-tight seal of the canal, retention of the tooth, and preservation of natural tooth function (36, 37). While the treatment success rate of conventional RCT has a reported range between 73% and 97% (38), ∼65% of the retreatment cases have been attributed to insufficient obturation (39). Retreatment of RCT (secondary RCT) as a treatment modality for a failed initial RCT has resulted in a lower success rate of 78.2% (38). While tooth extraction and implant placement are alternatives to RCT, endodontically treated natural teeth maintain proprioception and physiologic tooth mobility, while implants do not (40). Furthermore, patients with systemic medical conditions, such as uncontrolled diabetes or osteoporosis treated with i.v. bisphosphonates, have increased risk factors for implant survival (41, 42). Therefore, an improved obturation material may play an important role in preventing reinfection of root canals and enhance tooth retention.

The current standard material for RCT obturation is gutta percha (GP), an inert thermoplastic polymer that is composed of the GP latex, zinc oxide, a radiopacifier to allow for clinical X-ray imaging to monitor treatment progress, and a plasticizer (43). Conventional GP, while frequently used, has previously been associated with microleakage, allowing oral fluids and bacteria to access the treated root canal, and suboptimal mechanical properties with respect to handling the material, potentially resulting in buckling during obturation, among others (44, 45). Alternatives to conventional GP include obturation polymers that utilize dentin bonding to reduce the likelihood of failures due to leakage. However, insufficient evidence for enhanced treatment outcome and complications in handling the materials have led to limited clinical use (46). In addition, several studies have compared GP devices containing antibiotics, such as tetracycline and iodoform (47, 48). However, due to limited evidence and the potential for rapid burst release of the drug, these devices have also experienced limited use (48).

Challenges associated with conventional GP administration may be overcome through the incorporation of NDs. The present study harnessed the combined chemical, mechanical, and architectural properties of NDs to clinically validate a nanodiamond–gutta percha composite (NDGP) as a root canal filling material (Fig. 1*A*). Importantly, the NDGP demonstrated improved tensile strength and resistance to elongation compared with unmodified GP, while retaining similar handling properties to those of unmodified GP for clinical use such as unimpaired loading into the obturation system (Fig. 1 *B* and *C*) and extrusion (Fig. 1*D*). In addition, while assessing the potential therapeutic contributions of the NDs was not a primary endpoint of the study, the root canal obturation with NDGP did not impair periapical healing compared with unmodified GP after conventional RCT. In addition, no reinfections were reported for the three NDGP-treated patients. As such, the findings from this small cohort progress report support the equivalence of NDGP to unmodified GP, as well as the potential for NDGP to enhance clinical treatment outcomes incorporating functionalized NDs with antimicrobial agents. Furthermore, this study provides an in-human evaluation of the clinical tolerance of detonation ND particles, serving as an important foundation for the continued translation of NDs toward therapeutic applications.

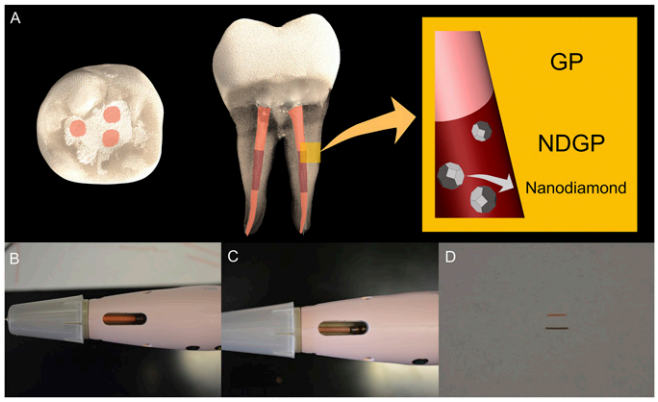

Fig. 1. NDGP clinical presentation. (*A*) Top–down view and side view of NDGP in the middle third of the root canal and unmodified GP in the apical and coronal thirds of the root canal-treated tooth. (*B*) Top–down view of unmodified GP in the dispensing unit. (*C*) Top–down view of NDGP in the dispensing unit. (*D*) Extruded unmodified GP (top) and NDGP (bottom).

Results

Thermogravimetric Analysis, Radiopacity, and Mechanical Properties of NDGP. Thermogravimetric analysis (TGA) spectra of unmodified GP and NDGP (5 wt% ND) are shown in Fig. 2*A*. Of note, the 15–17% weight loss of NDGP and GP observed between 100 °C and 400 °C was attributed to polymer and organic moiety (e.g., stearic acid) decomposition. At ∼500–550 °C, the NDs underwent an oxidation reaction, leading to carbon dioxide formation. Therefore, the weight loss observed between 500 °C and 800 °C is indirectly attributed to the amount of ND particles embedded in the NDGP. Furthermore, at a temperature of over 800 °C, both the unmodified GP and the NDGP had large-weight percentages of residue, 79–83% and 74–77%, respectively. The large-weight percentages of residue suggest the presence of large quantities of ZnO and $BaSO_4$ residues that did not undergo further decomposition.

During endodontic clinical procedures, root canal fillers need to be visualized by the clinician to monitor the progress of root canal obturation and ensure complete obturation by minimizing void spaces, where bacteria can reside. Therefore, to visualize the root canal filler, radiopacity is a critical property required of root canal filling materials. As shown in Fig. 2*B*, we evaluated the digital X-ray images of GP (top) and NDGP (bottom), which showed that both materials had equivalent radiopacity qualities.

To characterize the effects of ND incorporation into GP, we evaluated the mechanical strength properties such as stress–strain curve (Fig. 2*C*), elastic modulus (Fig. 2*D*), tensile strength (Fig. 2*E*), 0.2% offset yield strength (Fig. 2*F*), and percentage of elongation of NDGP compared with those of conventional GP (Fig. 2*G*). By incorporating NDs, the mechanical properties of the NDGP polymer composite were enhanced because of the high surface area to volume ratio of NDs, which increased the interface area between the polymer matrix and the reinforcement phase.

The elastic moduli of the NDGP samples were obtained from the elastic region, the initial straight portion of stress–strain curve, which is referred to as the stiffness of the material (Fig. 2*C*). As shown in Fig. 2*D*, the mean value of the elastic modulus of NDGP (120 ± 28.3 MPa) was not substantially changed compared with unmodified GP (167 ± 23.6 MPa). This demonstrated that the high content of hard inorganic moieties (confirmed to be over 79% from TGA), compared with the relatively small portion (14–16%) of soft organic polymer in the original GP sample, did not substantially alter the bulk material properties, thus mitigating the need to change the clinical handling protocols of NDGP. The NDGP (5 wt% ND) tensile strength (5.8 ± 0.20 MPa) was slightly increased compared with the unmodified GP tensile strength

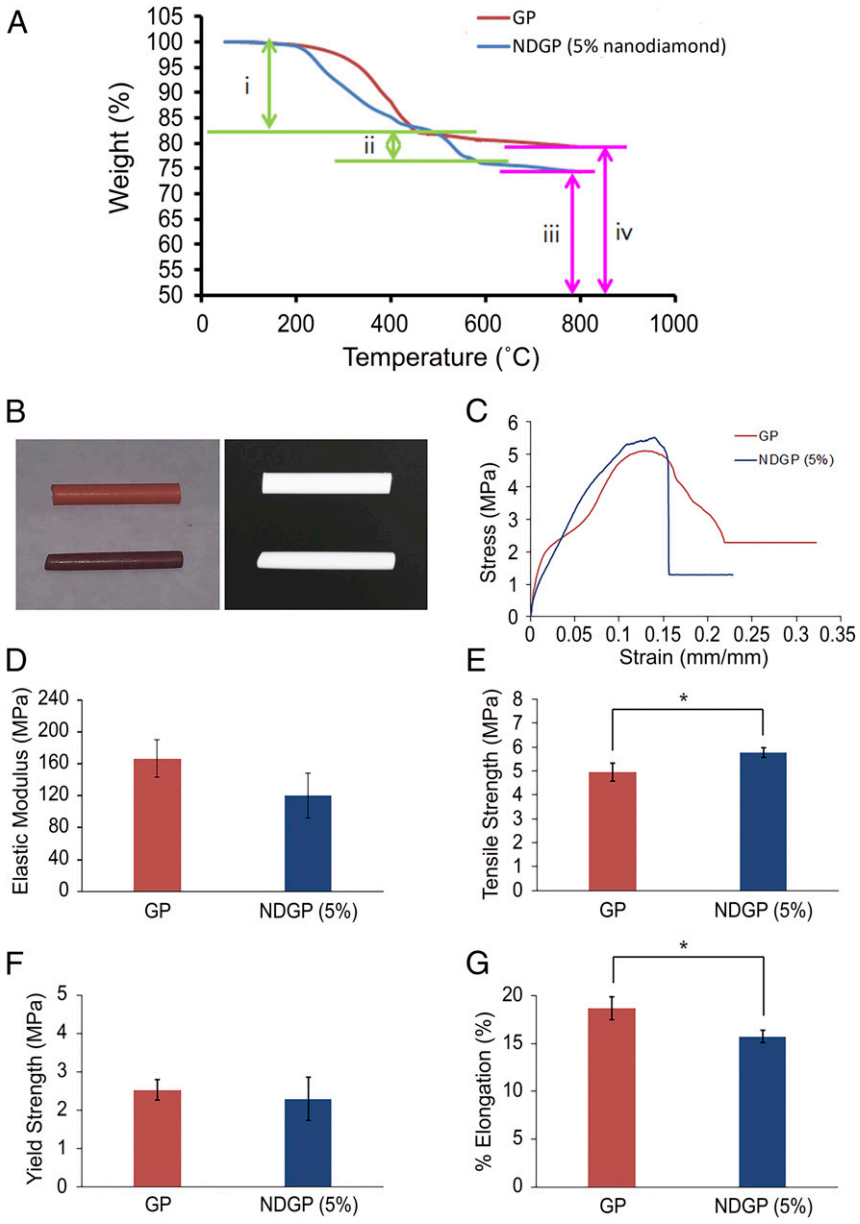

Fig. 2. Thermogravimetric analysis and mechanical properties comparisons between the unmodified GP product and the 5% NDGP. (*A*) Thermodiagram of the GP and NDGP. (*A*, *i*) Decrease in wt% of GP and NDGP is attributed to the polymer decomposition and organic moiety. (*A*, *ii*) The amount of decomposed ND is equal to the amount of ND incorporated into the NDGP. (*A*, *iii* and *iv*) $BaSO_4$ and ZnO residues left after the thermal decompositions. (*B*, *Left*) Image of GP (top) and NDGP (bottom) pellets. (*B*, *Right*) Digital X-ray image of GP (top) and NDGP (bottom) pellets. (*C*) Stress–strain curves from the measurement of tensile strength of GP and NDGP (5 wt% ND). (*D*) Elastic moduli of GP (167 ± 23.6 MPa) and NDGP with 5 wt% of ND (120 ± 28.3 MPa). Elastic moduli were calculated from the elastic region, the initial linear part of the stress–strain curves. Data are described as mean ± SD ($n = 3$), P value = 0.15. (*E*) Tensile strengths, the highest stress point of the stress–strain curve, for GP (4.9 ± 0.38 MPa) and NDGP with 5 wt% of ND (5.8 ± 0.20 MPa). Data are described as mean ± SD; *P value = 0.049 ($n = 3$). (*F*) The 0.2% offset yield strength of GP (2.5 ± 0.27 MPa) and NDGP with 5 wt% of ND (2.3 ± 0.57 MPa) measured from stress testing were correlated to the intersections of a stress–strain curve and projected straight lines, which were parallel to the initial straight portion of the stress–strain curve. The correlations explain the elastic limits of GP and NDGP. Data are described as mean ± SD ($n = 3$), P value = 0.63. (*G*) Percentages of elongation of GP (18.6 ± 1.18%) and NDGP with 5 wt% of ND (15.7 ± 0.660%) were calculated from comparing the change in length with the length of the original material. Data are described as mean ± SD; *P value = 0.04 ($n = 3$).

(4.9 ± 0.38 MPa) (Fig. 2*E*). The 0.2% offset yield strengths of GP (2.5 ± 0.27 MPa) and NDGP with 5 wt% of ND (2.3 ± 0.57 MPa) were not significantly different, indicating similar ductility or plasticity between the two materials (Fig. 2*F*). Additionally, the percentage of elongation of NDGP was decreased (15.7 ± 0.660%) compared with that of unmodified GP (18.6 ± 1.18%) (Fig. 2*G*). Therefore, the NDGP thermoplastic material exhibited improved tensile strength while retaining similar ductility in comparison with that of unmodified GP, which resulted in an unaltered obturation procedure for the clinician.

RCT Overview. An access opening was made to enter the pulp chamber. Using endodontic files, infected and/or necrotic pulp tissue was removed from the root canals. The canals were then cleaned and shaped to create a suitable space for root canal obturation. Frequent irrigation with a disinfecting solution (4%

NaOCl) eliminated residual bacteria that may have remained in the small accessory canals, which are often hard to address solely with mechanical debridement or the removal of damaged tissue. The root filling, or obturation process, was then conducted to seal the canal space in an effort to prevent reinfection (Fig. 3). Obturation was performed by placing a GP master cone to create a tight seal at the apical end of the tooth with zinc oxide eugenol (ZOE) sealer (Fig. 3*A*). Preserving the apical seal, excess GP was seared off with a heated instrument (Fig. 3*B*), and the remaining GP was condensed further (Fig. 3*C*). After the apical seal was made with the master cone, the respective root canal treatment protocols for the treatment arms (control and NDGP) were implemented. For the control patient (C1), additional GP material was delivered into the remaining canal space, for both the middle third (Fig. 3*D*) and the coronal third (Fig. 3*E*), and then condensed to complete the obturation (Fig. 3*F* and Movie S1). For the NDGP patients (ND1, ND2, and ND3), NDGP was delivered into the middle third of the canal space (Fig. 3*G*), and unmodified GP was extruded into the coronal third (Fig. 3*H*) of the canal space to complete the obturation (Fig. 3*I* and Movie S2). Once the canals were sufficiently obturated, a final restoration, e.g., a crown or filling, was then placed on the tooth to prevent coronal leakage into the canals.

C1. C1 is a 72-y-old male with medical history that included hypertension, diabetes mellitus, and hypercholesterolemia; however, C1 did not report taking any medications (Table 1). C1 reported spontaneous pain (comparative pain scale: 8 of 10) in the region around the upper left premolar. Upon clinical assessment at the initial appointment, C1 did not report pain or sensitivity during both the biting/releasing and cold tests, in which cold stimulus was applied to the tooth and surrounding teeth to test for vitality and patient response. C1 was tender to percussion, which involved tapping the tooth to test for patient sensitivity. The tooth was diagnosed with pulpal necrosis and asymptomatic apical periodontitis (AAP), resulting in apical bone loss that could be identified radiographically. C1's pretreatment radiograph (Fig. 4*A*) revealed a periapical radiolucency (PARL), which is a lesion of infected bone tissue, surrounding the root of tooth 13 (upper left premolar). C1's radiographs showed the existence of a PARL at pretreatment (Fig. 4*A*), the completed obturation (Fig. 4*B*), and 6-mo follow-up (Fig. 4*C*) and were measured for C1's PARL diameters (Fig. 4*D*), shown in the expanded view of the pretreatment (Fig. 4*E*) and 6-mo follow-up (Fig. 4*F*) radiographs. A PARL diameter of 5.07 mm was confirmed on the initial radiograph taken before treatment (Fig. 4*E*).

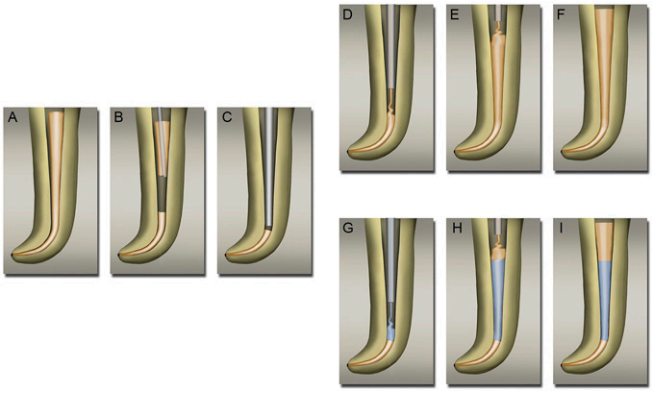

Fig. 3. Control and NDGP obturation process. (*A*) Master GP cone placed with zinc-eugenol sealer. (*B*) Removal of excess GP with heated plugger. (*C*) Condensing master GP to apical 5 mm. (*D*) Canal space filled with GP, using extruder starting from apical end. (*E*) Canal space filled with unmodified GP up to cervical third. (*F*) Fully condensed and completed obturation with unmodified GP. (*G*) Middle third of the canal space was filled with NDGP, using extruder that started from the apical end. (*H*) Cervical third of the canal space was filled with unmodified GP. (*I*) Fully condensed and completed obturation with NDGP in the middle third of the canal.

Treatment of C1 involved cleaning and shaping of the canal, which included removal of the infected pulp tissue. On the day of the initial appointment, a coronal access was created in tooth 13 and the clinician placed an intracanal medicament, calcium hydroxide paste, in the canal to disinfect the root canal space. The access was temporarily sealed for 1 wk up until the second appointment. During the second visit, root canal obturation on tooth 13 as well as a temporary restoration was successfully completed.

At the 6-mo follow-up appointment, C1 reported no subjective symptoms and presented no swelling or tenderness to palpation or percussion. Additionally, C1's radiographs indicated a reduction in the PARL diameter (4.19 mm) (Fig. 4*F*) compared with the preoperative PARL diameter of 5.07 mm (Fig. 4*E*). A permanent composite restoration was placed on tooth 13 to seal the access opening. Furthermore, the clinician determined that tooth 13 was showing signs of healing and would continue to be monitored for complete recovery.

ND1. ND1 is a 55-y-old female and was taking an unspecified antifungal medication for an ear infection at the time of treatment (Table 1). ND1 was diagnosed with pulpal necrosis and AAP, and ND1 reported pain from tooth 27 (lower right canine) that had lasted for 14 d (comparative pain scale: 5 of 10) that was subsequently alleviated during the treatment appointment. The symptoms were provoked with palpation on the gingiva around the tooth and managed with ibuprofen. Upon clinical assessment at the treatment appointment, ND1 did not report any pain associated with the tooth upon administering cold and biting/releasing tests, but did report tenderness to percussion. RCT was successfully performed on tooth 27, which included rubber dam placement (Fig. 5*A*), creation of access cavity (Fig. 5*B*), and obturation (Fig. 5*C*) with no reported complications. Following the RCT, tooth 27 was restored with a glass ionomer base followed by an amalgam restoration over the access opening (Fig. 5*D*). ND1 did not report any pain following the first appointment. ND1's radiographs showed the existence of a PARL at pretreatment (Fig. 5*E*), the completed obturation (Fig. 5*F*), 3-mo follow-up (Fig. 5*G*), and 6-mo follow-up (Fig. 5*H*) and were measured for ND1's PARL diameters (Fig. 5*I*), shown in the expanded view of the pretreatment (Fig. 5*J*), 3-mo follow-up (Fig. 5*K*), and 6-mo follow-up (Fig. 5*L*) radiographs. Preoperative radiographs of tooth 27 revealed a PARL diameter of 3.56 mm (Fig. 5*J*).

At the 3-mo follow-up, ND1 was asymptomatic with no adverse events. Additionally, ND1's periapical radiograph indicated osseous healing (PARL diameter of 2.81 mm) (Fig. 5*K*), compared with preoperative PARL diameter of 3.56 mm (Fig. 5*J*).

At the 6-mo follow-up, ND1 was asymptomatic, and the clinical evaluations of the patient were all within normal limits. ND1 did not respond to palpation or percussion of tooth 27, and ND1's radiographs indicated a PARL diameter of 2.48 mm (Fig. 5*L*). It was determined that healing was complete.

ND2. ND2 is a 92-y-old male currently taking Synthroid (thyroid hormone) for hypothyroidism (Table 1). ND2 previously experienced aching, spontaneous pain (comparative pain scale: 9 of 10) adjacent to tooth 6, the upper right canine (Fig. 6*A*), for 2 wk before the initial appointment. ND2 also reported pain upon biting, reportedly lasting all day and throughout the night, and used over-the-counter medications to alleviate the pain that was subsequently alleviated by the procedure. On the day of the procedure, patient ND2 presented with pulpal necrosis and an extraoral facial swelling. ND2 did not respond to cold testing upon clinical examination, reported pain upon biting/releasing,

Table 1. Patient demographic, health history, and treatment summary

ID	C1	ND1	ND2	ND3
Age, y	72	55	92	54
Gender	Male	Female	Male	Male
Tooth	13 (upper left premolar)	27 (lower right canine)	6 (upper right canine)	23 (lower left incisor)
Medical history	Hypertension, diabetes, hypercholesterolemia, no prescription medications reported	No major medical conditions reported	Taking synthroid (thyroid hormone) for hypothyroidism	Taking Triumeq (HIV/AIDS treatment)
Diagnosis	Pulp necrosis/AAP	Pulp necrosis/AAP	Pulp necrosis/chronic apical abscess	Pulp necrosis/AAP
Preoperative characteristics	History of spontaneous pain	History of pain reported	Spontaneous pain	No pain reported
Operative issues	No complications reported	No complications reported	No complications reported	No complications reported
Postoperative characteristics	No pain or symptoms reported	No pain or symptoms reported	No pain or symptoms reported	No pain or symptoms reported
3-mo follow-up	NA	No pain or symptoms reported	No pain or symptoms reported	NA
6-mo follow-up	No pain or symptoms reported	No pain or symptoms reported	—	—

NA, not analyzed.

and was tender to percussion. A PARL of endodontic origin was seen around tooth 6 on the preoperative radiographs.

Incision and drainage of the abscess were completed, and the tooth was accessed for intracanal debridement and disinfection with calcium hydroxide (Fig. 6*B*). On the subsequent visit, RCT was successfully performed on tooth 6 with no reported complications or posttreatment symptoms following the appointment. ND2's radiographs showed the existence of a PARL at pretreatment (Fig. 6*C*), the completed obturation (Fig. 6*D*), and 3-mo follow-up (Fig. 6*E*) and were measured for ND2's PARL diameters (Fig. 6*F*), shown in the expanded view of the pretreatment (Fig. 6*G*) and 3-mo follow-up (Fig. 6*H*) radiographs. The pretreatment PARL diameter was measured to be 3.45 mm as shown in Fig. 6*G*. ND2 was asymptomatic as he did not experience any pain after the procedure (comparative pain scale: 0 of 10), and a permanent restoration was placed into the access.

At the 3-mo follow-up, ND2 was asymptomatic and had no reported adverse events. Additionally, ND2's radiographs indicated a smaller PARL diameter of 2.63 mm (Fig. 6*H*), which showed a reduction from the initial preoperative PARL diameter

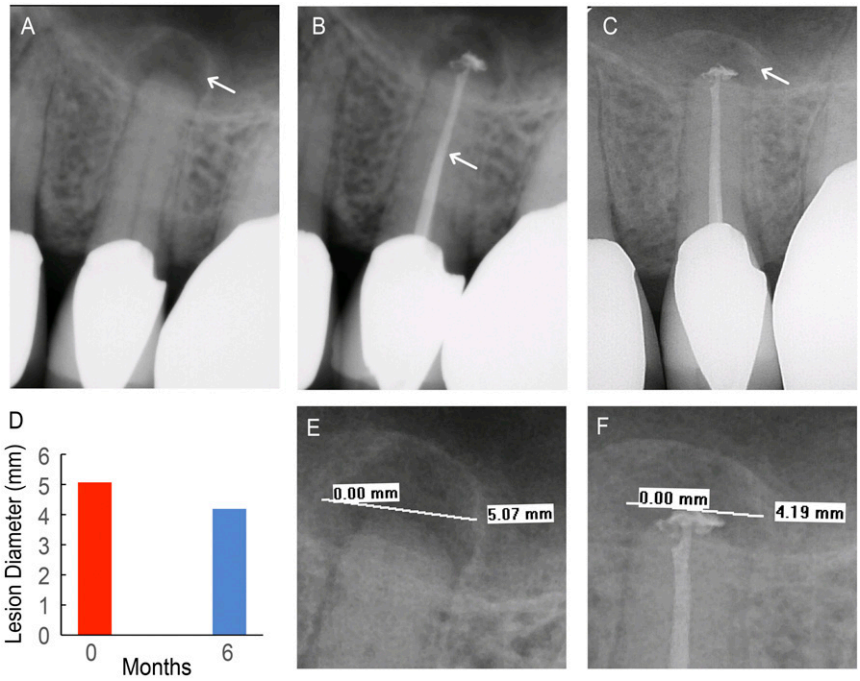

Fig. 4. Control patient (C1). (*A*) Pretreatment radiograph of tooth 13 with existing apical lesion (white arrow). (*B*) Completed backfill (white arrow) and apical seal with unmodified GP. (*C*) Six-month follow-up radiograph shows the apical lesion with increased bone density (white arrow). (*D*) Lesion diameter at pretreatment (red) and 6-mo follow-up (blue) appointments. (*E*) A 5.07-mm apical lesion diameter was visible on the pretreatment radiograph. (*F*) A 4.19-mm apical lesion diameter was visible on the 6-mo follow-up radiograph.

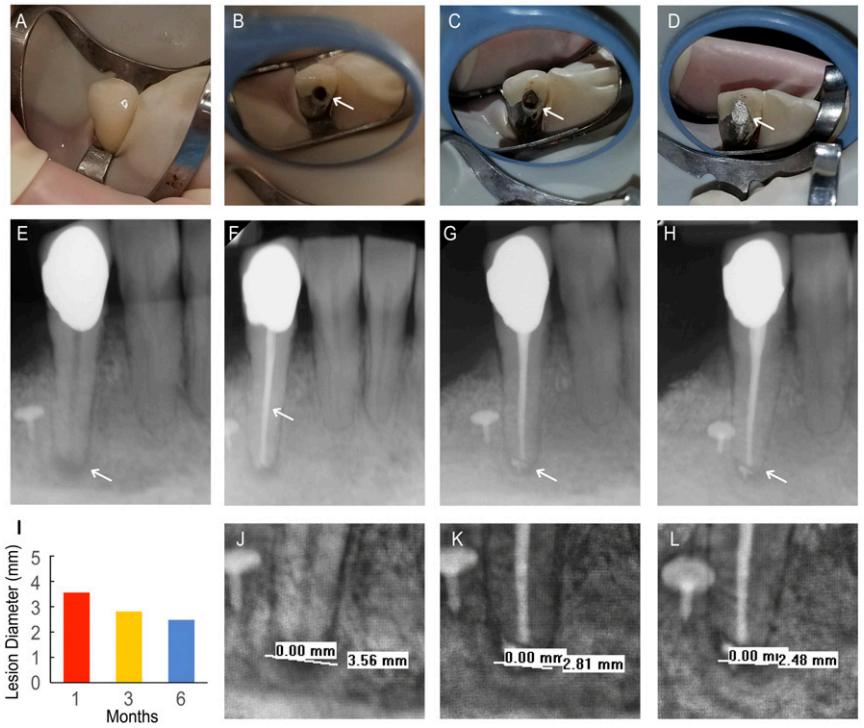

Fig. 5. NDGP-treated patient 1 (ND1). (*A*) Pretreatment clinical image of tooth 27 taken after rubber dam placement. (*B*) Clinical image of access cavity (white arrow) before obturation. (*C*) Clinical image of completed obturation visible through access cavity (white arrow). (*D*) Clinical image of coronal restoration sealing access cavity (white arrow). (*E*) Pretreatment radiograph with periapical lesion (white arrow). (*F*) Completed obturation with unmodified GP apical seal, NDGP backfill, and unmodified GP coronal seal. (*G*) Three-month follow-up radiograph with healing periapical lesion (white arrow). (*H*) Six-month follow-up radiograph with healing periapical lesion. (*I*) Lesion diameter at pretreatment, 3-mo, and 6-mo follow-up appointments. (*J*) A 3.56-mm lesion was visible on pretreatment radiograph. (*K*) A 2.81-mm lesion diameter was visible on the 3-mo follow-up appointment. (*L*) A 2.48-mm lesion diameter was visible on the 6-mo follow-up appointment.

of 3.45 mm (Fig. 6*G*). Tooth 6 was restored with a glass ionomer base and full-coverage crown. It was determined that tooth 6 was currently healing and would continue to be monitored for complete recovery.

ND3. ND3 was a 54-y-old male with HIV infection under antiretroviral treatment with Triumeq (abacavir, dolutegravir, and lamivudine) (Table 1). ND3 did not report any preoperative symptoms (comparative pain scale: 0 of 10). Tooth 23 was not responsive to cold testing, biting/releasing, or percussion, yielding a diagnosis of pulpal necrosis and AAP.

RCT was performed on tooth 23, which included rubber dam placement (Fig. 7*A*), creation of access cavity (Fig. 7*B*), and obturation (Fig. 7*C*). ND3's radiographs showed the existence of a PARL at pretreatment (Fig. 7*D*) and the completed obturation (Fig. 7*E*), which are shown in the expanded view of the pretreatment (Fig. 7*F*). Preoperative radiographs of tooth 23 revealed a PARL diameter of 3.53 mm (Fig. 7*F*).

The RCT procedure was completed on tooth 23, with no reported treatment complications during instrumentation, shaping, and obturation (Fig. 7*E*). ND3 did not report any symptoms (comparative pain scale: 0 of 10) following the treatment. Patient ND3 has not reported any postoperative symptoms or complications indicative of root canal reinfection and is on schedule for follow-up.

Discussion

Conventional GP is the standard filling material for root canal obturation as it provides an adequate seal, can be distinguished from natural tooth structure on radiographs, and can be retrieved or removed if necessary (49). Despite these favorable qualities, conventional GP obturation can still lead to endodontic failures due to reinfection of root canals, which are in part associated with microleakage. As such, conventional GP may be conducive to bacterial regrowth should the bacterial remnants in the root canal space and the tissue fluid reestablish contact. As previously mentioned, insufficient obturation is associated with a higher likelihood of an unfavorable prognosis of retreatment cases (39). Furthermore, a large cross-sectional study of 1,030 endodontically treated teeth found a 43.7% incidence of apical periodontitis when there was inadequate endodontic obturation, while 17.7% of comprehensively obturated teeth were diseased (50). Conventional obturation materials are not utilized for mechanical reinforcement of the tooth structure following RCT. However, in terms of benefits offered by NDGP compared with unmodified GP, the enhanced mechanical properties of the NDGP that were validated by the tensile strength studies can potentially improve clinician handling to increase the likelihood of a dense obturation, which may provide technical advantages in the obturation procedure for clinicians (51). In addition to tensile strength evaluation, this study completed a function-based evaluation of mechanical properties of NDGP and unmodified GP that included a stress–strain curve, an elastic modulus, 0.2% offset yield strength, and percentage of elongation analyses. These other mechanical function-based evaluations were important in demonstrating the equivalent or better clinician handling properties of NDGP compared with those of unmodified GP, which is critical for clinical implementation and translation of NDs and more specifically NDGP. Furthermore, the elastic modulus, 0.2% offset yield strength, and percentage of elongation were quantitative measures of plasticity and/or

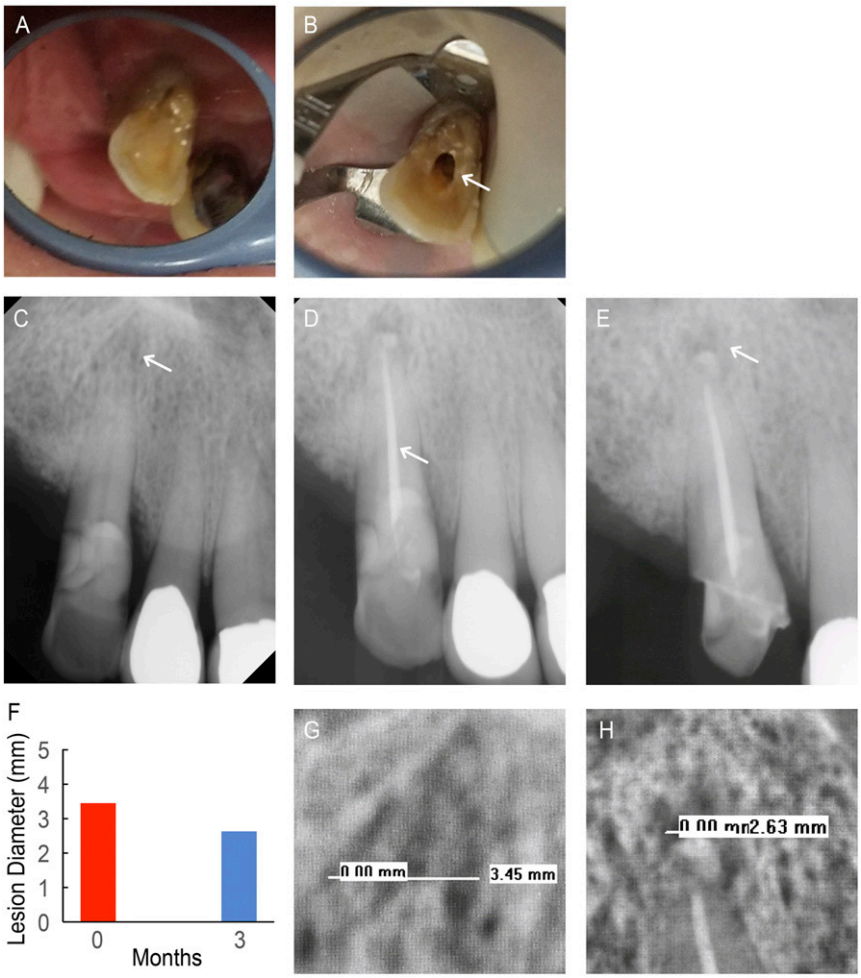

Fig. 6. NDGP-treated patient 2 (ND2). (*A*) Pretreatment clinical image of tooth 6. (*B*) Clinical image of access cavity (white arrow). (*C*) Pretreatment radiograph with existing periapical lesion (white arrow). (*D*) Completed obturation with unmodified GP apical seal, NDGP backfill, and unmodified GP coronal seal (white arrow). (*E*) Three-month follow-up radiograph with healing periapical lesion (white arrow). (*F*) Lesion diameter at pretreatment (red) and 3-mo follow-up (blue) appointments. (*G*) The 3.45-mm lesion diameter was visible on the pretreatment radiograph. (*H*) The 2.63-mm lesion diameter was visible on the 3-mo follow-up radiograph.

ductility affecting the clinician's ability to manipulate, shape, and extrude the NDGP in the tooth's root canal.

The field of nanomedicine has started to make important clinical advances in recent years, with in-human trials being conducted to assess material safety, as well as applications toward drug delivery, imaging/diagnostics, and biomaterials engineering (3, 5, 8, 9, 52–55). In these and forthcoming clinical studies, nanoparticles have been injected for systemic therapy/imaging using small molecules, RNA interference, and additional emerging approaches (Clinicaltrial.gov identifiers NCT03086278 and NCT00503906). Scaffolds with enhanced properties are also being explored to promote tissue repair (Clinicaltrial.gov identifier NCT02305602). Among these promising approaches, NDs have received increasing attention due to their combination of uniquely faceted electrostatic properties. These properties have mediated remarkably potent drug binding and sustained elution for indications ranging from oncology to wound repair and synergistic coordination of surrounding water molecules to realize among the highest ever reported contrast imaging efficiencies, as well as composites with improved mechanical properties for potential regenerative medicine and tissue engineering applications (13, 15, 56). Studies have shown that NDs are well tolerated in comprehensive preclinical and large animal studies (28, 57). Importantly, NDs with consistent particle size and surface chemistry properties can be scalably synthesized, supporting their clinical translation (17, 26, 58).

This clinical progress report addressed the current challenges associated with RCT, which is a pervasive issue in oral health. RCT failure may lead to tooth extraction, requiring more invasive procedures that may involve implant placement. Due to side effects from RCT reinfection that can lead to periapical bone loss and/or infection, additional disciplines outside of oral health including orthopedic surgery and infectious diseases can also be impacted by the need for improved RCT materials (59, 60). Therefore, this progress report introduced a unique in-human validation of detonation NDs, using the NDGP platform. As shown in Fig. 2, NDGP synthesis was shown to be scalable, resulting in improved mechanical properties compared with unmodified GP with no apparent impairment to radiopacity and the clinical procedures required for NDGP administration. Importantly, endodontic failure can be attributed to procedural errors that can occur during the shaping, cleaning, and obturation procedures (61). No reported procedural errors occurred during endodontic treatment for our NDGP trial that could have led to complications, demonstrating the clinical relevance of NDGP. As it has been established that void spaces lead to root canal reinfection, prior preclinical NDGP obturation studies that served as a foundation for this clinical trial assessed the presence

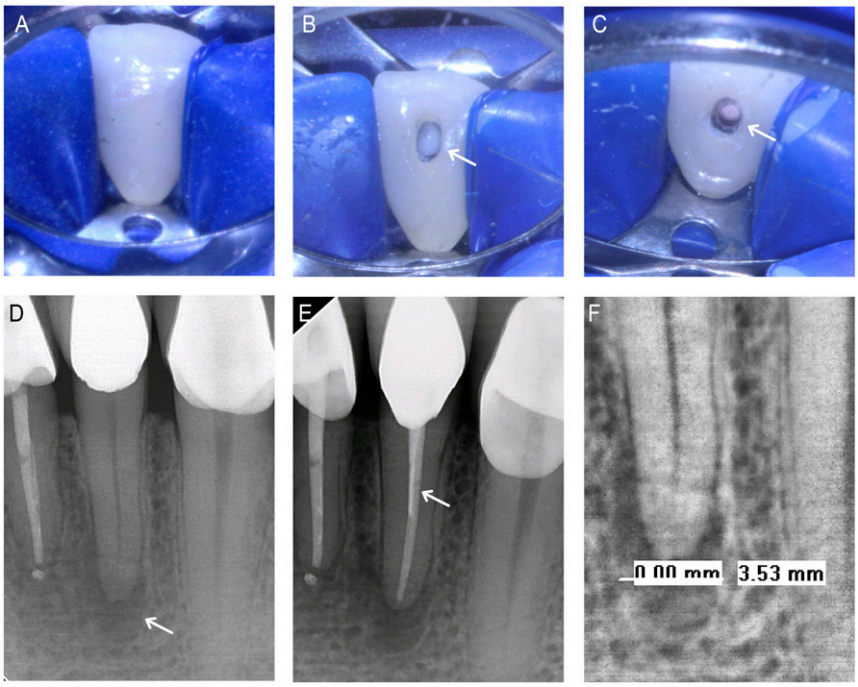

Fig. 7. NDGP-treated patient 3 (ND3). (*A*) Pretreatment clinical image of tooth 23. (*B*) Clinical image of access cavity (white arrow). (*C*) Clinical image of completed obturation (white arrow). (*D*) Pretreatment radiograph with existing periapical lesion (white arrow). (*E*) Completed obturation with unmodified GP apical seal, NDGP backfill, and unmodified GP coronal seal (white arrow). (*F*) The 3.53-mm pretreatment lesion diameter.

of voids via microcomputed tomography imaging (micro-CT) to obtain high-resolution analysis of NDGP obturation efficiency (31). This progress report confirmed that NDGP-mediated obturation resulted in no apparent increase in void spaces compared with that of unmodified GP (31). As shown in our clinical trial, when evaluating and comparing the radiographs of ND1, ND2, and ND3 postobturation, the extent of obturation was deemed to be equivalent, at minimum, to those realized through GP-based procedures such as that for C1.

Based on the potential reduction of void spaces or reduced incidence of coronal leakage using NDGP vs. unmodified GP, the primary endpoint of this study was to monitor and confirm the absence of apical periodontitis during the course of an equivalence study between NDGP and unmodified GP. Importantly, prior studies have shown that inadequate RCT was more predictive of apical periodontitis than the absence of a crown as a coronal restoration (62, 63). While this progress report was based on three treatment-arm patients and one control-arm patient, retreatment was not indicated for ND1, ND2, or ND3 during the course of the progress report, supporting the continued recruitment of patients into the study.

Of note, the delivery of NDs alone was previously reported to mediate antimicrobial activity (64). However, the potential therapeutic contributions of the NDs were not considered as trial endpoints. The initial study results strongly indicate that the trial's primary endpoint will be met. This in turn would support the additional evaluation of ND-mediated drug loading and innate antimicrobial effects of the NDs as future trial endpoints. It should be mentioned that current medicated GP products have demonstrated inconsistent drug potency over time due to burst elution (48). In addition, previous studies have shown that residual bacteria can reside in additional canals even after the RCT procedure (65). This makes contact-mediated inhibition using NDGP a potentially viable alternative to current approaches.

The secondary trial endpoint assessed the absence of pain following RCT and the absence of symptoms upon clinical examination. C1 had a history of preoperative spontaneous pain, ND1 reported pain, ND2 reported a history of spontaneous and aching pain, and ND3 reported no pain. After treatment with the NDGP, all patients reported no pain or symptoms on the postoperative survey, 3-mo follow-up, and/or the 6-mo follow-up for ND1, ND2, and ND3.

As discussed previously, there have been many attempts to address the problem of RCT reinfection. However, substantial enhancements in preventing reinfection can be realized utilizing potential therapeutic properties of NDGP. In a previous study, NDs were used to sequester amoxicillin for contact-mediated bacterial inhibition, which could substantially reduce the risk of reinfection following RCT (31). The antimicrobial properties of drug-incorporated NDGP could potentially reduce the incidence of reinfection after the mechanical debridement and sealing are complete. Furthermore, recent advancements in drug optimization technologies have shown that NDs can be used for combination therapy, markedly enhancing therapeutic efficacy and reducing toxicity through the systematic and mechanism-independent design of ND-functionalized multidrug treatment (66–68). Importantly, these technology platforms have also been clinically validated (69).

Assessing the potential impact of increasing the ND wt% in NDGP may serve as a foundation for the future assessment of unmodified ND-mediated antimicrobial activity using NDGP. This may lead to additional efforts to modulate ND content in coordination with drug loading to simultaneously optimize the therapeutic efficacy and mechanical properties of drug-functionalized NDGP. In addition, there is a need to conduct additional studies where the entire root canal is obturated with NDGP. Of note, as NDGP continues to be evaluated in the reported trial, future regulatory compliance will be sought to expand the types of studies that can be conducted with NDGP. It is also important to note that this study served as a progress report. With regard to the sample size, this work discussed the treatment outcomes of three NDGP-arm patients and one control-arm patient. While the assessment of more patients will facilitate the statistical evaluation of study

outcomes, these progress report findings support the continued patient recruitment and subsequent and adequately powered studies to assess the impact of ND-mediated therapy to prevent reinfection in comparison with conventional, unmodified GP.

The administration of NDGP simultaneously confers the beneficial properties of GP with the added benefit of increased mechanical strength and potential for ND-mediated antimicrobial and/or pharmacologic antimicrobial activity into treated canals. These capabilities may reduce the risk of RCT reinfection, improving long-term treatment outcomes for a large number of patients requiring endodontic therapies. In this equivalence study progress report, the clinical administration of NDGP was evaluated in comparison with unmodified GP. The study was designed to be interventional for the purpose of treatment, with patient recruitment randomized, single-blinded masking and a control arm and treatment arm. At the 3-mo and/or 6-mo follow-up appointments with ND1, ND2, and C1, the size of the periapical lesions decreased by 1.08 mm, 0.82 mm, and 0.88 mm, respectively. The decrease in the periapical radiolucency size may indicate that the lesion is healing as new bone is reforming (70). These studies demonstrate the promise of NDGP and ND particles as clinically applicable platforms for drug delivery, imaging, and composite biomaterials for a broad spectrum of indications.

Materials and Methods

Study Design. This study was conducted following patient informed consent and enrollment based on a trial protocol approved by the University of California, Los Angeles (UCLA) Institutional Review Board (IRB) under IRB protocol 15-002015 and was assigned a Clinicaltrials.gov identifier NCT02698163, as an interventional study with a primary purpose of treatment. Four patients were enrolled in the NDGP trial and randomized into two groups: NDGP embedded with 5 wt% ND particles (ND1, ND2, and ND3) and unmodified gutta percha (C1). The study was approved for 30 patients in total, with 15 in each treatment arm, and as such is still ongoing.

Standard protocol for RCT was performed following the American Dental Association Guidelines and that of the UCLA School of Dentistry Section of Endodontics. Patients' signs, symptoms, and objective findings were assessed after recruitment into the study, via an administered survey. Qualifying patients were referred to the study's clinical principal investigators and were selected for informed consent, single-blinded randomization, and participation if they were 18 y old or older. Exclusion criteria for the study included prior endodontic treatment on the referred tooth, osteoporosis medication or i.v. bisphosphonates, dental material allergies, required prophylaxis, severely medically compromised, and congenital/developmental disorders.

RCT Procedure. All procedures were performed using local anesthesia and rubber dam isolation. RCT included drilling into the tooth to obtain ideal access into the pulpal chamber, and the infected pulpal tissues were cleaned out using endodontic files.

All canals were irrigated and disinfected with 4% Clorox Sodium Hypochlorite (The Clorox Company) and dried. Using the Apex Locator (Root ZX II; J. Morita Mfg. Corp.), the operator found and confirmed the working length, or length of the canal, and RC-Prep (Premier) was used to lubricate the canals during the filing portion of the procedures. As determined by the operator, calcium hydroxide was used as an interappointment antibiotic if required at the time of the appointment. The ZOE sealer (Kerr Corporation) was placed at the apex of the roots, and the root canal was obturated using the vertical condensation technique.

Obturation was performed by placing a GP master cone at the apical end of the tooth to create a tight seal. While preserving the apical seal, excess GP was seared off with a heated instrument, and the remaining GP was condensed further. All root canals were filled with standard root canal filler material GP at the apical third (GT Gutta-Percha; Dentsply Tulsa Dental Specialties), filled with either unmodified GP (Dental Gutta Percha; Obtura Spartan Endodontics) or ND-reinforced GP in the middle third, and filled with unmodified GP (Obtura Spartan Endodontics) in the coronal third. Once the canals were sufficiently obturated, a final restoration, such as a crown or composite/amalgam, was then placed on the tooth to prevent reinfection of the canal. Following the RCT, 3-mo and/or 6-mo follow-up assessments were conducted to check for the healing of lesions in the periapical bone.

The primary outcome measure of the study was the reduction of apical periodontitis, which was verified with a radiograph of the treated tooth after 3 mo and/or 6 mo posttreatment. These radiographs were compared with the radiograph of the treated tooth taken before the RCT procedure. The primary outcome was assessed via digital radiographs with size 1 or 2 XDR Digital Intraoral Sensors (XDR Radiology). The images were then transferred digitally and evaluated for the periapical lesion size. All radiographs were analyzed preoperatively, postoperatively, and 3 mo and/or 6 mo following the procedure. If a periapical lesion was detected, then the clinicians used the ruler tool in the XDR program to measure the largest diameter of the radiographic lesion.

The secondary outcome measures included assessing changes in postoperative pain. Pain was assessed via a postoperative survey and a clinical examination.

Materials. ND stock solution (50 mg/mL) was batch analyzed, obtained from the NanoCarbon Research Institute Co., Ltd., a dedicated ND processing and characterization facility, and sterilized before the experiments. Unmodified GP was purchased from Obtura Spartan Endodontics. For the purposes of NDGP synthesis, Eucalyptol ($C_{10}H_{18}O$) and absolute ethanol were purchased from Sigma-Aldrich.

Synthesis and Characterization of NDGP. The NDGP was synthesized by mixing raw GP and ND. First, with eucalyptol as a solvent, raw GP materials (0.3–0.4 g) were dispersed at a ratio of 1:32 of raw GP material to eucalyptol, which was followed by 30 min of sonication. After thoroughly dispersing the raw GP materials, 5% (wt/wt) of ND solution (H_2O:ethanol was 1:2) was added and dispersed by sonication, followed by overnight lyophilization until all of the solvents were removed. After lyophilization, solid NDGP was heated and pelletized at 90–110 °C for the purpose of loading into an endodontic obturation system. To verify the composition of the NDGP, thermogravimetric analysis was performed. The experiment was conducted on the Pyris Diamond TG/DTA (PerkinElmer Inc.) in an air environment with 20 mL/min flow rate. During TG/DTA measurement, changes in weight were recorded from 50 °C to 800 °C at a 5 °C/min heating rate.

To measure the mechanical properties of GP and NDGP, the tensile strength test was performed using an Instron Universal Testing Machine (Model 5564; Instron). The tests were pursued with a 0.3-cm/min strain rate and with sample gauge lengths of 0.89–0.9 cm. The cross-sectional area was calculated from each sample's diameter, and the elastic modulus was calculated from the elastic region, the initial straight portion of the stress–strain curve. For the comparison with NDGP, GP was prepared with the same procedure but without the addition of ND particles.

Statistical Analysis. For the analysis of the elastic moduli, tensile strength, and percentage of elongation properties of the NDGP, a two-tailed Student's *t* test was used. α was set at 0.05, and P values <0.05 were considered statistically significant. All tests were performed in triplicate, and statistical analyses were conducted using MATLAB R2014a (MathWorks Inc.).

Data Availability. Reagents are available upon request by contacting the corresponding authors of this study.

ACKNOWLEDGMENTS. The authors thank the patients and their families for their participation in this trial. The authors also thank Dr. Daniel A. Choi for helpful discussions. E.K.-H.C. acknowledges support from the National Research Foundation Cancer Science Institute of Singapore Research Centres of Excellence (RCE) Main Grant and Ministry of Education Academic Research Fund (MOE AcRF) (Tier 2 MOE2015-T2-2-126). This work is funded by the National University Cancer Institute (NCIS) Yong Siew Yoon Research Grant through donations from the Yong Loo Lin Trust. E.C.S. gratefully acknowledges the United Cerebral Palsy of Los Angeles Endowed Chair in Special Patient Care. M.K.K. gratefully acknowledges the Jack A. Weichman Chair in Endodontics. D. Ho acknowledges support from the National Science Foundation Early Career Faculty Development Program (CAREER) Award (CMMI-1350197), the Center for Scalable and Integrated NanoManufacturing (DMI-0327077), CMMI-0856492, DMR-1343991, OISE-1444100, the V Foundation for Cancer Research Scholars Award, a Wallace H. Coulter Foundation Translational Research Award, the National Cancer Institute (NCI) (U54CA151880), the Society for Laboratory Automation and Screening Endowed Fellowship, and Beckman Coulter Life Sciences. The content is solely the responsibility of the authors and does not necessarily represent the official views of the NCI or the National Institutes of Health.

1. Peppas NA, Hilt JZ, Khademhosseini A, Langer R (2006) Hydrogels in biology and medicine: From molecular principles to bionanotechnology. *Adv Mater* 18:1345–1360.
2. Farokhzad OC, et al. (2006) Targeted nanoparticle-aptamer bioconjugates for cancer chemotherapy in vivo. *Proc Natl Acad Sci USA* 103:6315–6320.
3. Bae Y, Fukushima S, Harada A, Kataoka K (2003) Design of environment-sensitive supramolecular assemblies for intracellular drug delivery: Polymeric micelles that are responsive to intracellular pH change. *Angew Chem Int Ed Engl* 42:4640–4643.
4. Qian C, et al. (2016) Light-activated hypoxia-responsive nanocarriers for enhanced anticancer therapy. *Adv Mater* 28:3313–3320.
5. Jensen SA, et al. (2013) Spherical nucleic acid nanoparticle conjugates as an RNAi-based therapy for glioblastoma. *Sci Transl Med* 5:209ra152.
6. Pun SH, Davis ME (2002) Development of a nonviral gene delivery vehicle for systemic application. *Bioconjug Chem* 13:630–639.
7. Peer D, et al. (2007) Nanocarriers as an emerging platform for cancer therapy. *Nat Nanotechnol* 2:751–760.
8. Hrkach J, et al. (2012) Preclinical development and clinical translation of a PSMA-targeted docetaxel nanoparticle with a differentiated pharmacological profile. *Sci Transl Med* 4:128ra139.
9. Davis ME, et al. (2010) Evidence of RNAi in humans from systemically administered siRNA via targeted nanoparticles. *Nature* 464:1067–1070.
10. Huang H, Pierstorff E, Osawa E, Ho D (2007) Active nanodiamond hydrogels for chemotherapeutic delivery. *Nano Lett* 7:3305–3314.
11. Lam R, et al. (2008) Nanodiamond-embedded microfilm devices for localized chemotherapeutic elution. *ACS Nano* 2:2095–2102.
12. Huang H, Pierstorff E, Osawa E, Ho D (2008) Protein-mediated assembly of nanodiamond hydrogels into a biocompatible and biofunctional multilayer nanofilm. *ACS Nano* 2:203–212.
13. Manus LM, et al. (2010) Gd(III)-nanodiamond conjugates for MRI contrast enhancement. *Nano Lett* 10:484–489.
14. Chen M, et al. (2009) Nanodiamond-mediated delivery of water-insoluble therapeutics. *ACS Nano* 3:2016–2022.
15. Chow EK, et al. (2011) Nanodiamond therapeutic delivery agents mediate enhanced chemoresistant tumor treatment. *Sci Transl Med* 3:73ra21.
16. Zhang X-Q, et al. (2011) Multimodal nanodiamond drug delivery carriers for selective targeting, imaging, and enhanced chemotherapeutic efficacy. *Adv Mater* 23: 4770–4775.
17. Mochalin VN, Shenderova O, Ho D, Gogotsi Y (2011) The properties and applications of nanodiamonds. *Nat Nanotechnol* 7:11–23.
18. Chow EK-H, Ho D (2013) Cancer nanomedicine: From drug delivery to imaging. *Sci Transl Med* 5:216rv4.
19. Moore LK, Chow EK-H, Osawa E, Bishop JM, Ho D (2013) Diamond-lipid hybrids enhance chemotherapeutic tolerance and mediate tumor regression. *Adv Mater* 25: 3532–3541.
20. Wang X, et al. (2014) Epirubicin-adsorbed nanodiamonds kill chemoresistant hepatic cancer stem cells. *ACS Nano* 8:12151–12166.
21. Hou W, et al. (2017) Nanodiamond-manganese dual mode MRI contrast agents for enhanced liver tumor detection. *Nanomedicine* 13:783–793.
22. Barnard AS, Ōsawa E (2014) The impact of structural polydispersivity on the surface electrostatic potential of nanodiamond. *Nanoscale* 6:1188–1194.
23. Lai L, Barnard AS (2011) Stability of nanodiamond surfaces exposed to N, NH, and NH2. *J Phys Chem C* 115:6218–6228.
24. Lai L, Barnard AS (2011) Modeling the thermostability of surface functionalisation by oxygen, hydroxyl, and water on nanodiamonds. *Nanoscale* 3:2566–2575.
25. Krueger A (2008) The structure and reactivity of nanoscale diamond. *J Mater Chem* 18:1485.
26. Liang Y, Ozawa M, Krueger A (2009) A general procedure to functionalize agglomerating nanoparticles demonstrated on nanodiamond. *ACS Nano* 3:2288–2296.
27. Zhang Q, et al. (2011) Fluorescent PLLA-nanodiamond composites for bone tissue engineering. *Biomaterials* 32:87–94.
28. Moore L, et al. (2016) Biocompatibility assessment of detonation nanodiamond in non-human primates and rats using histological, hematologic, and urine analysis. *ACS Nano* 10:7385–7400.
29. Khanal M, et al. (2015) Selective antimicrobial and antibiofilm disrupting properties of functionalized diamond nanoparticles against Escherichia coli and Staphylococcus aureus. *Part Part Syst Charact* 32:822–830.
30. Wehling J, Dringen R, Zare RN, Maas M, Rezwan K (2014) Bactericidal activity of partially oxidized nanodiamonds. *ACS Nano* 8:6475–6483.
31. Lee D-K, et al. (2015) Nanodiamond-gutta percha composite biomaterials for root canal therapy. *ACS Nano* 9:11490–11501.
32. Kim H-J, Zhang K, Moore L, Ho D (2014) Diamond nanogel-embedded contact lenses mediate lysozyme-dependent therapeutic release. *ACS Nano* 8:2998–3005.
33. Law AS, Durand EU, Rindal DB, Nixdorf DR; DPBRN Group (2010) "Doctor, why does my tooth still hurt"? *Northwest Dent* 89:33–36.
34. Sundqvist G, Figdor D (1998) *Endodontic Treatment of Apical Periodontitis. Essential Endodontology* (Blackwell, Oxford), pp 242–277.
35. Orstavik D (2008) *Essential Endodontology: Prevention and Treatment of Apical Periodontitis* (Blackwell Munksgaard, Copenhagen).
36. Estrela C, et al. (2014) Characterization of successful root canal treatment. *Braz Dent J* 25:3–11.
37. Salehrabi R, Rotstein I (2004) Endodontic treatment outcomes in a large patient population in the USA: An epidemiological study. *J Endod* 30:846–850.
38. Elemam RF, Pretty I (2011) Comparison of the success rate of endodontic treatment and implant treatment. *ISRN Dent* 2011:640509.
39. Hoen MM, Pink FE (2002) Contemporary endodontic retreatments: An analysis based on clinical treatment findings. *J Endod* 28:834–836.
40. Grieznis L, Apse P, Blumfelds L (2010) Passive tactile sensibility of teeth and osseointegrated dental implants in the maxilla. *Stomatologija* 12:80–86.
41. Naujokat H, Kunzendorf B, Wiltfang J (2016) Dental implants and diabetes mellitus-a systematic review. *Int J Implant Dent* 2:5.
42. Mattheos N, Caldwell P, Petcu EB, Ivanovski S, Reher P (2013) Dental implant placement with bone augmentation in a patient who received intravenous bisphosphonate treatment for osteoporosis. *J Can Dent Assoc* 79:d2.
43. Friedman CM, Sandrik JL, Heuer MA, Rapp GW (1975) Composition and mechanical properties of gutta-percha endodontic points. *J Dent Res* 54:921–925.
44. Clinton K, Van Himel T (2001) Comparison of a warm gutta-percha obturation technique and lateral condensation. *J Endod* 27:692–695.
45. Soo WK, Thong YL, Gutmann JL (2015) A comparison of four gutta-percha filling techniques in simulated C-shaped canals. *Int Endod J* 48:736–746.
46. Lotfi M, et al. (2013) Resilon: A comprehensive literature review. *J Dent Res Dent Clin Dent Prospect* 7:119–130.
47. Melker KB, Vertucci FJ, Rojas MF, Progulske-Fox A, Bélanger M (2006) Antimicrobial efficacy of medicated root canal filling materials. *J Endod* 32:148–151.
48. Rathke A, Meisohle D, Bokelmann J, Haller B (2012) Antibacterial activity of calcium hydroxide and chlorhexidine containing points against Fusobacterium nucleatum and Parvimonas micra. *Eur J Dent* 6:434–439.
49. Grossman LLI, Oliet S, Del Rio CE (1988) *Endodontic Practice* (Lea & Febiger, Philadelphia).
50. Song M, Park M, Lee C-Y, Kim E (2014) Periapical status related to the quality of coronal restorations and root fillings in a Korean population. *J Endod* 40:182–186.
51. Shashidhar J, Shashidhar C (2014) Gutta percha verses resilon: An *in vitro* comparison of fracture resistance in endodontically treated teeth. *J Indian Soc Pedod Prev Dent* 32:53–57.
52. Sykes EA, et al. (2016) Tailoring nanoparticle designs to target cancer based on tumor pathophysiology. *Proc Natl Acad Sci USA* 113:E1142–E1151.
53. Lu Y, Aimetti AA, Langer R, Gu Z (2016) Bioresponsive materials. *Nat Rev Mater* 2: 16075.
54. Deng ZJ, et al. (2013) Layer-by-layer nanoparticles for systemic codelivery of an anticancer drug and siRNA for potential triple-negative breast cancer treatment. *ACS Nano* 7:9571–9584.
55. Meng H, et al. (2013) Two-wave nanotherapy to target the stroma and optimize gemcitabine delivery to a human pancreatic cancer model in mice. *ACS Nano* 7: 10048–10065.
56. Rammohan N, et al. (2016) Nanodiamond-gadolinium(III) aggregates for tracking cancer growth in vivo at high field. *Nano Lett* 16:7551–7564.
57. Moore L, et al. (2014) Comprehensive interrogation of the cellular response to fluorescent, detonation and functionalized nanodiamonds. *Nanoscale* 6:11712–11721.
58. Pentecost A, Gour S, Mochalin V, Knoke I, Gogotsi Y (2010) Deaggregation of nanodiamond powders using salt- and sugar-assisted milling. *ACS Appl Mater Interfaces* 2:3289–3294.
59. LaPorte DM, Waldman BJ, Mont MA, Hungerford DS (1999) Infections associated with dental procedures in total hip arthroplasty. *J Bone Joint Surg Br* 81:56–59.
60. Li X, Kolltveit KM, Tronstad L, Olsen I (2000) Systemic diseases caused by oral infection. *Clin Microbiol Rev* 13:547–558.
61. Tabassum S, Khan FR (2016) Failure of endodontic treatment: The usual suspects. *Eur J Dent* 10:144–147.
62. Kim S (2010) Prevalence of apical periodontitis of root canal-treated teeth and retrospective evaluation of symptom-related prognostic factors in an urban South Korean population. *Oral Surg Oral Med Oral Pathol Oral Radiol Endod* 110:795–799.
63. Siqueira JF, Jr, Rôças IN, Ricucci D, Hülsmann M (2014) Causes and management of post-treatment apical periodontitis. *Br Dent J* 216:305–312.
64. Khanal M, et al. (2015) Nanodiamonds: Selective antimicrobial and antibiofilm disrupting properties of functionalized diamond nanoparticles against Escherichia coli and Staphylococcus aureus. *Part Part Syst Charact* 32:791.
65. Nair PN (2006) On the causes of persistent apical periodontitis: A review. *Int Endod J* 39:249–281.
66. Wang H, et al. (2015) Mechanism-independent optimization of combinatorial nanodiamond and unmodified drug delivery using a phenotypically driven platform technology. *ACS Nano* 9:3332–3344.
67. Ho D, Zarrinpar A, Chow EK-H (2016) Diamonds, digital health, and drug development: Optimizing combinatorial nanomedicine. *ACS Nano* 10:9087–9092.
68. Ho D, Wang C-HK, Chow EK-H (2015) Nanodiamonds: The intersection of nanotechnology, drug development, and personalized medicine. *Sci Adv* 1:e1500439.
69. Zarrinpar A, et al. (2016) Individualizing liver transplant immunosuppression using a phenotypic personalized medicine platform. *Sci Transl Med* 8:333ra349.
70. Huumonen S, Orstavik D (2002) Radiological aspects of apical periodontitis. *Endod Topics* 1:3–25.